Deformation Mechanism in Graphene Nanoplatelet Reinforced Tantalum Carbide using High Load *In situ* Indentation

Cheng Zhang, Benjamin Boesl, Laura Silvestroni, Diletta Sciti, Arvind Agarwal

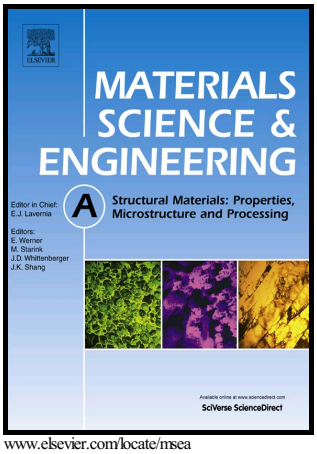

www.elsevier.com/locate/msea

PII: S0921-5093(16)30885-1
DOI: http://dx.doi.org/10.1016/j.msea.2016.07.110
Reference: MSA33941

To appear in: *Materials Science & Engineering A*

Received date: 22 May 2016
Revised date: 13 July 2016
Accepted date: 26 July 2016

Cite this article as: Cheng Zhang, Benjamin Boesl, Laura Silvestroni, Diletta Sciti and Arvind Agarwal, Deformation Mechanism in Graphene Nanoplatelet Reinforced Tantalum Carbide using High Load *In situ* Indentation, *Material Science & Engineering A,* http://dx.doi.org/10.1016/j.msea.2016.07.110

Deformation Mechanism in Graphene Nanoplatelet Reinforced Tantalum Carbide using High Load *In situ* Indentation

Cheng Zhang[1], Benjamin Boesl[1], Laura Silvestroni[2], Diletta Sciti[2], and Arvind Agarwal[1*]

[1]Plasma Forming Laboratory, Department of Mechanical and Materials Engineering, Florida International University, Miami, FL, 33174, USA
[2]Institute of Science and Technology for Ceramics (ISTEC), CNR-ISTEC Faenza, Via Granarolo, 64 - 48018 Faenza (RA), Italy

Abstract

High load *in-situ* indentation testing with real time SEM imaging was carried out on spark plasma sintered graphene nanoplatelets (GNP) reinforced TaC composites. The prime goal of this study was to understand the deformation behavior and the reinforcing mechanisms of GNPs. The results suggest that addition of GNPs had significant effect on dissipating indentation energy and confining the overall damage area to a localized region of TaC. The average crack length reduced by 26% whereas total damage area shrunk by 85% in TaC-5 vol.% GNP sample as compared to pure TaC. TEM analysis concluded that well dispersed GNPs result in a strong and clean interface between TaC and GNP with trace amount of amorphous layer that leads to improved energy dissipation mechanism.

Keywords: High load in situ indentation; Tantalum Carbide; Graphene nanoplatelets; damaged area; interface

1. Introduction

Tantalum carbide (TaC) with a melting point of 3880^{o}C is an ultra-high temperature ceramic, which possesses high Young's modulus (477-560 GPa) and high hardness (13.5-20 GPa) [1-4]. These properties make it attractive for applications such as rocket propulsion system, cutting tool, and wear-resistance parts. However, its low sinterability and low fracture toughness are major challenges in realizing the true potential of TaC. Sintering aids such as B_4C, carbon and transition metal disilicides are useful in consolidating TaC to near full densification [5]. In recent studies, nano B_4C, carbon nanotube (CNT) and graphene nanoplatelets (GNP) have been proven as effective sintering aids and reinforcing additives for TaC and other ceramics such as Si_3N_4 and SiC [6-14]. Attempts to improve the toughness by introduction of discontinuous phases, like SiC particles, platelets or randomly oriented fibers, resulted not efficacious probably owing to the negative effect of thermal residual stresses, due to the introduction of lower coefficient of thermal expansion (CTE) secondary phases [15]. Improved densification, fracture toughness, flexure strength and elastic modulus have been however reported with the addition of CNT and GNP to ceramic matrix [6-14]. In the most recent work, up to 5 vol. % graphene nanoplatelets (GNP) was incorporated in TaC and spark plasma sintered at 1850°C to understand its effect as sintering and toughening reinforcement. The relative density increased from 94.6% to 98.8% with increasing GNP content [11]. Also, the fracture toughness improved from 5.6 to 11.1 MPa $m^{1/2}$ with an increasing GNP content. Toughening mechanisms include GNP bending, sliding, crack bridging and crack deflection. Although the above listed studies [11,12] have provided a good understanding of the reinforcement mechanism provided by graphene nanoplatelets, the advent of *in-situ* mechanical testing inside an electron microscope has created an unprecedented opportunity to study and understand the deformation behavior in real time. Nowak et al. [16] performed *in-situ* nanoindenation tests on thin gold film deposited on a fused

quartz substrate and correlated the deformation mechanism with the variations in load-displacement curve in real time without making any assumptions. Kiani. et al [17] conducted an *in-situ* TEM based uniaxial compression test on TaC micropillars along (100) and (011) directions to understand the room –temperature plasticity of sub-micron-size TaC single crystals. Dislocations movement was observed at room temperature during compression of TaC micropillars with yield strength identified as 9 GPa for TaC (100) and 11 GPa for TaC (011). Typically, *in-situ* indentation tests are conducted at *low load* (micro or milli Newton) for understanding the deformation behavior of a single crystal or small volume [18-19]. In the case of polycrystalline and bulk composite materials, high load (several Newton) *in situ* indentation inside SEM can reveal the true deformation behavior and interaction among multiple phases, grains, porosity, and reinforcement. Recently, Rudolf et al. [20-21] carried out high load (~500 N) *in-situ* indentation tests on spark plasma sintered GNP pellets inside SEM. It was concluded that toughening mechanisms provided by GNPs are orientation dependent where out-of-plane direction can dissipate 270% more energy than in-plane direction.

Inspired by this scenario, we report high load *in-situ* SEM indentation behavior of spark plasma sintered TaC-GNP composites synthesized in our previous study [11]. Load displacement curves for varying GNP concentration in TaC are obtained. The damage in TaC-GNP composites is quantified in terms of residual damage zone. SEM videos are recorded during the indentation tests to visualize the occurrence of deformation and fracturing in TaC. The reinforcement effect provided by GNP is elucidated in real time.

2. Experimental details

2.1 Materials

The starting tantalum carbide (TaC) powder (Inframat Advanced Materials LLC, Connecticut, USA) has an average particle size of 0.36± 0.13 µm. The purity of the tantalum carbide powder by weight is 99.7%. Impurities include free carbon (< 0.15%), oxygen (0.15-0.3%), and niobium (<0.3%). The Ta to C ratio is approximately 1:1. Graphene nanoplatelets (xGNP-M-5, XG Science, Lansing, MI, USA) have an average of thickness of 6-14 nm suggesting 20-40 sheets of graphene in each GNP. GNP particles have an average diameter of 15 µm and a relative surface area of 120-150 m^2/g.

2.2 Powder Mixing and Synthesis

TaC-GNP composites were prepared with four different GNP content *viz.* 0, 1, 3, and 5 vol.%. These samples have been named as pure TaC, TaC-1G, TaC-3G, and TaC-5G respectively. Powder mixtures were made by wet chemistry method. GNP was first ultrasonicated in acetone for 90 min to reduce the agglomeration. TaC powder was then added into GNP solution and ultrasonicated for another 60 min. TaC- GNP solution was placed inside an oven at 80^{o}C for 24 hour to drying. Dried mixed powders were then sintered using 10-4 spark plasma sintering machine (GT Advanced Technologies, Santa Rosa, CA, USA). The mixed powder was placed inside a 20 mm diameter die wrapped with a thin graphite foil. Two punches were inserted from top and bottom to seal the powders. Graphite foil was also placed between punches and powder for easy removal after sintering. Samples were sintered at 1850^{o}C with a

heating rate of 200^{o}C/min and a pressure of 80-100 MPa [11]. The holding time was 10 min and the environment in the chamber consisted of Argon gas at a pressure of 3-6.5 Pa.

2.3 Microstructure analysis

TaC-GNP composites were cut and polished to 1 μm and were analyzed with scanning electron microscopy (FE-SEM, Carl Zeiss Sigma NTS GmbH, Oberkochen, Germany) coupled with energy dispersive spectroscopy (EDS, X-Act, INCA Energy 300, Oxford Instruments, Abingdon, UK).

TEM samples were prepared by cutting 3 mm disks from the sintered pellets using a wire EDM. These were mechanically ground down to about 150 μm and then further ion beam thinned until small perforations were observed by optical microscopy. Local phase analysis was performed using transmission electron microscopy (FEI Tecnai F20 ST), with an acceleration voltage of 200 keV, equipped with an energy-dispersive X-ray system (EDAX EDS X-ray spectrometer PV9761) with super ultra-thin window.

2.4 *In-situ* Indentation

High load *in-situ* indentation was carried out inside a dual beam Focused Ion Beam/SEM (JIB-4500, JEOL, Ltd. Japan). A linear, screw driven micro-load frame (SEM Tester 1000, MTI Instruments Inc. USA) attached a 1 μm, 120^{o} conospherical tip was employed for the indentation testing. Indentation tests were carried out on polished surfaces at a maximum applied load of 500 N at a loading and unloading rate of 100 N/min. The dwell time at maximum load was 5 minutes.

Load-displacement curves and corresponding SEM videos in real time showing deformation behavior were recorded.

3. Results

3.1 Microstructure and Mechanical Properties of TaC-GNP Composites

A brief summary of microstructure and mechanical properties of TaC-GNP composites is provided here for the sake of complete understanding (Table 1) [11]. The relative density increased from ~95% up to 99% with increasing GNP content from 0 to 5 vol.% indicating GNP serves as sintering aid in TaC consolidation.. Pure TaC presented areas of localized porosity, whilst with the progressive introduction of GNPs, the porosity decreased. GNP agglomerates were visible only in compositions with volume amount above 3%, whilst in TaC-1G it was difficult to identify the graphene sheets, Fig. 1a-c. The GNPs sheets tended to align in the direction perpendicular to the applied pressure and on the polished surface it could be seen that besides large GNP agglomerates, thin sheets were found at TaC grain boundaries, Fig. 1d. In composites TaC-3G and -5G, the GNPs were found to wrap groups of grain and exhibited pulled out on the fracture surface, Fig. 1e-f.

Micro-hardness decreased after adding GNP into TaC owing to the lower hardness of graphene compared with TaC. Fracture toughness increased with the addition of GNP up to 99%. Reinforcing mechanisms included crack bridging, GNP pull-out, GNP sheet sliding, and GNP kinking that dissipated energy [11].

Table 1. Mechanical Properties of TaC-GNP Composites

Sample	Relative Density (%)	Micro-hardness (GPa)	Indentation toughness (MPa $m^{1/2}$)
Pure TaC	94.6±0.7	18.9±3.4	5.6±1.8
TaC-1G	96.9±0.4	16.5±1.8	8.3±1.8
TaC-3G	97.5±0.4	14.1±1.6	7.7±1.9
TaC-5G	98.8±0.2	12.9±1.4	11.1±2.4

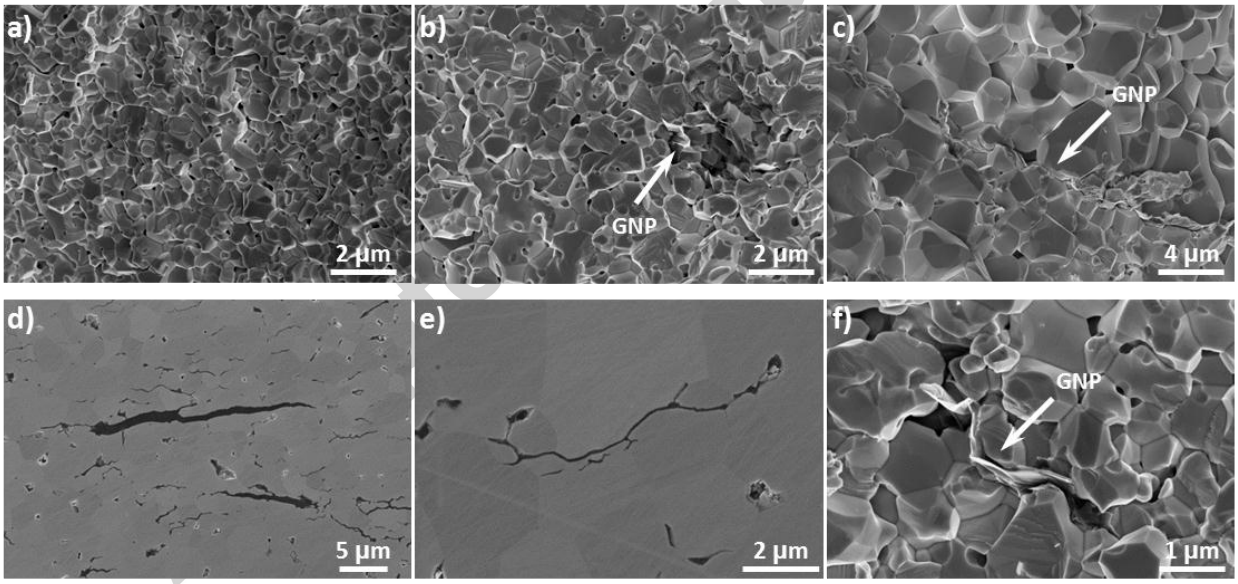

Figure 1: SEM images of TaC composites containing a) 1, b) 3 and c) 5 vol.% GNPs. d)-e) Polished surface of TaC-5G showing different size of the graphene sheets, f) fracture surface of TaC-3G showing GNP wrapped around the grains and pulled-out.

TEM analyses were performed on TaC-5G and showed that the GNPs sheets tended to pack on each other, Fig. 2a, but the graphene structure was preserved despite the high sintering

temperature, as demonstrated in the high resolution TEM image and the electron diffraction pattern in Fig. 2b. Figure 2d shows GNP sandwiched between TaC grains and EDS spectra from the interface shows presence of C and trace amount of oxygen, whereas EDS from the matrix grains show presence of only Ta and C, suggesting that the GNP could have cleaned the matrix powder during sintering from oxygen contamination and thus enhanced the densification. TaC/TaC interfaces were generally found to be clean of amorphous phases, Fig. 2c, whilst the investigation of TaC/GNP grain boundary revealed mixed behavior. A high magnification image of the interface in Figure 2e shows a thin (1-2 nm) amorphous layer between TaC-GNPs. On the other hand, Figure 2f shows a very clean and distinct interface between TaC and GNP without any amorphous layer.

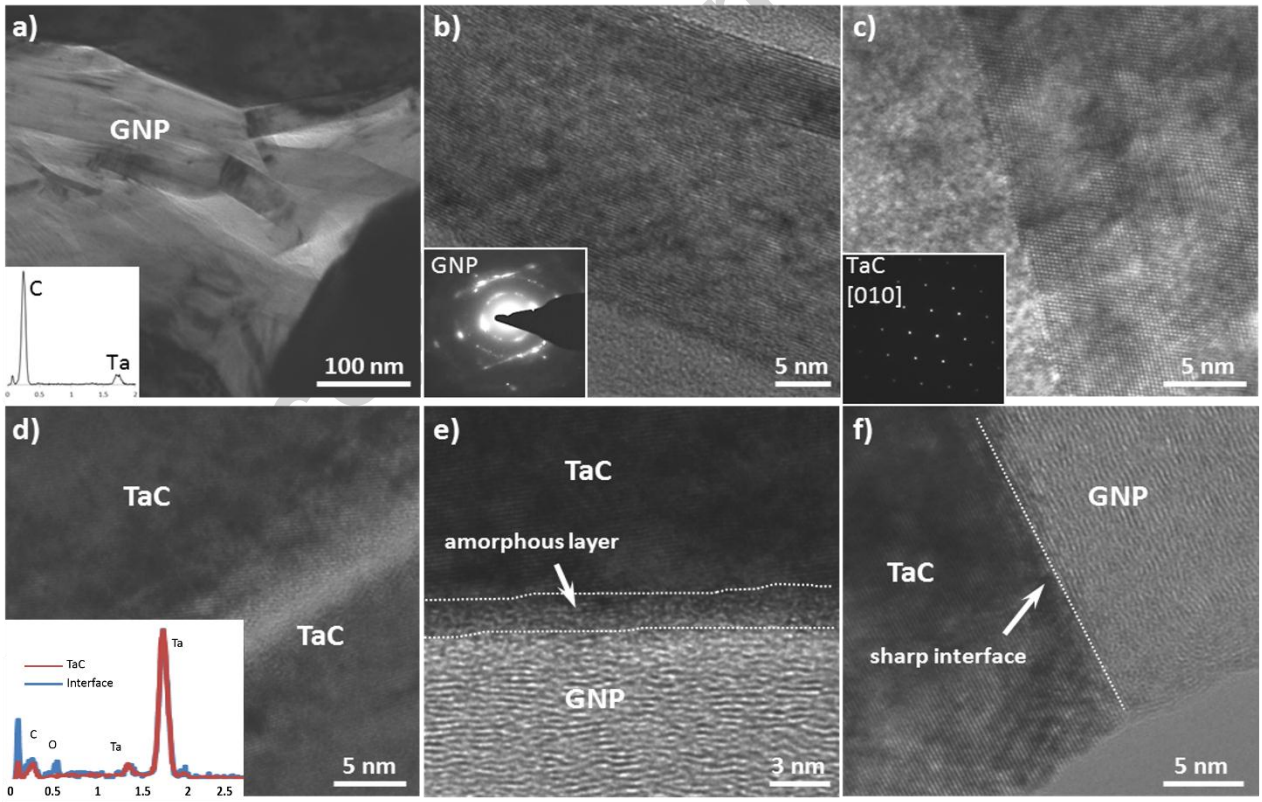

Figure 2: TEM images of TaC composites containing 5 vol% GNPs. GNPs at a) low magnification and b) high resolution with EDS spectrum and diffraction pattern inset. c) HR-TEM image showing clean typical TaC/TaC interface; d) TEM image and EDS spectra on the interface of TaC-GNP sandwiched structure

showing partially oxidized graphene. HRTEM images showing the different interface type between TaC and GNP (e) with amorphous phase or (f) clean.

3.2 *In situ* Indentation Load-Displacement Behavior

Figure 3 shows load-displacement behavior of pure TaC and TaC-5G samples during high load indentation tests inside SEM. Pure TaC and TaC-5G had similar final displacement and the unloading curves of these two samples were also largely alike. However, the loading curves were quite different for TaC and TaC-5G samples. There was a slope change when the load reached 95N in pure TaC sample. According to real-time SEM videos, the slope change in pure TaC was due to the energy dissipating mechanism shifted from grain slipping to crack propagation. TaC-5G sample displayed few spikes (marked 3) in the loading curve with change in the slopes in intermediate regions and these were attributed to grain slipping which will be elaborated in the next section.

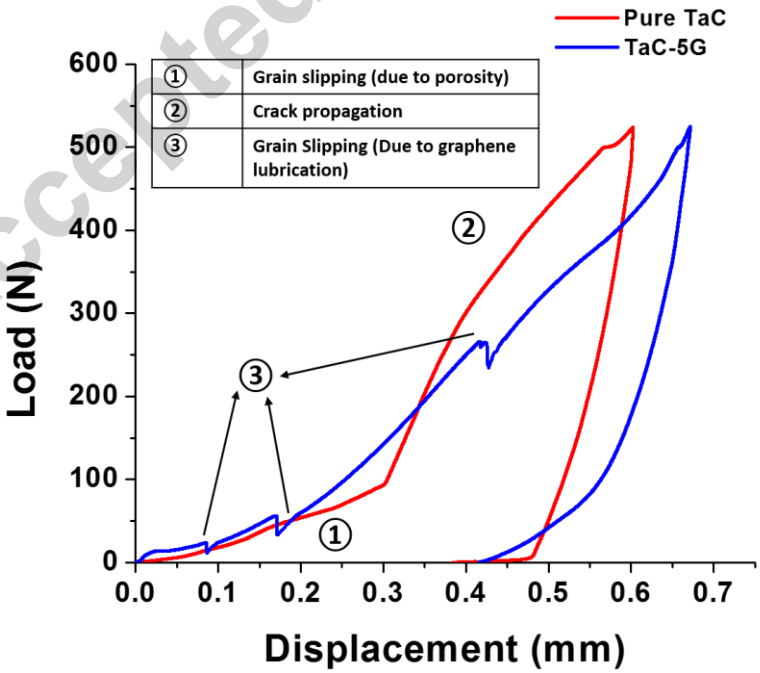

Figure 3. Load-displacement curves for TaC-GNP indentation tests

The extent of damage caused by high load indentation was measured by the total "impact area" which is defined as the sum of residual indent area and the area subtend by radical cracks. Figure 4 illustrates the methodology to estimate total impact area due to indentation damage. Figure 5 shows a comparison of total impact areas for TaC samples with varying GNP concentration. The results are also listed in Table 2. The total impact area (i.e. damaged area) shrunk significantly from pure TaC to composites with increasing volume amount of GNP, i.e. for TaC-1G, TaC-3G and TaC-5G decreased by 21.7%, 39.3% and 68.5%, respectively. It is evident that the addition of graphene nanoplatelets has great effects on limiting the total impact area and hence improving materials endurance.

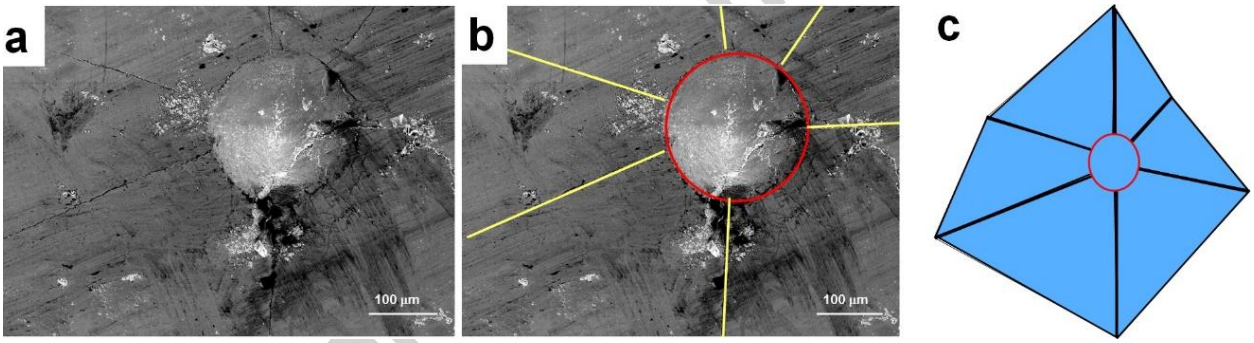

Figure 4. Schematic to illustrate the total impact area estimation after high load indentation. (a) Top view of the residual indent with cracks, (b) measurement of the crack lengths, and (c) connecting all cracks provides an estimation of total impact (damaged) area due to high load indentation

Table 2. Summary of Indentation Crack Features and Impact Area for TaC-GNP Composites

Sample	Residual indent area (mm^2)	Number of major cracks	Average crack length(mm)	Total impact area (mm^2)
Pure TaC	0.19	6	0.61±0.18	1.36
TaC-1G	0.18	5	0.61±0.15	1.06
TaC-3G	0.16	4	0.57±0.26	0.64
TaC-5G	0.13	3	0.45±0.17	0.20

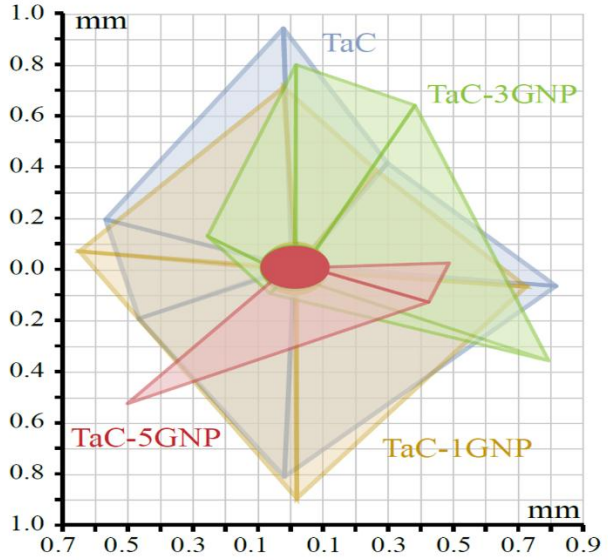

Figure 5. Comparison of total impact areas of TaC samples reinforced with GNPs.

Post indentation residual indents were analyzed by SEM, as Figure 6. In detail, Figure 6a displays the residual indent for pure TaC with chipping and long cracks; similarly, Figure 6b shows a smooth indent for TaC-1G, but with reduced or no chipping. Unlike pure TaC and TaC-1G samples, TaC-3G (Figure 6c) and TaC-5G (Figure 6d) show rough indents with severe fracture in the indent region. However, this damage was highly localized (e.g. chipping and liftoff) as cracks originating from TaC-3G and TaC-5G were very small and barely visible as compared to TaC and TaC-1G samples. Table 2 shows the number and average length of cracks which reduced from pure TaC to TaC-5G. The average crack length shortened by 26.9%, and major cracks has been eliminated by 50% with an increasing GNP content. The area of residual indents also decreased with an increasing GNP content from 0.192 mm^2 for pure TaC to 0.129 mm^2 for TaC-5G (Table 2 and Figure 5).

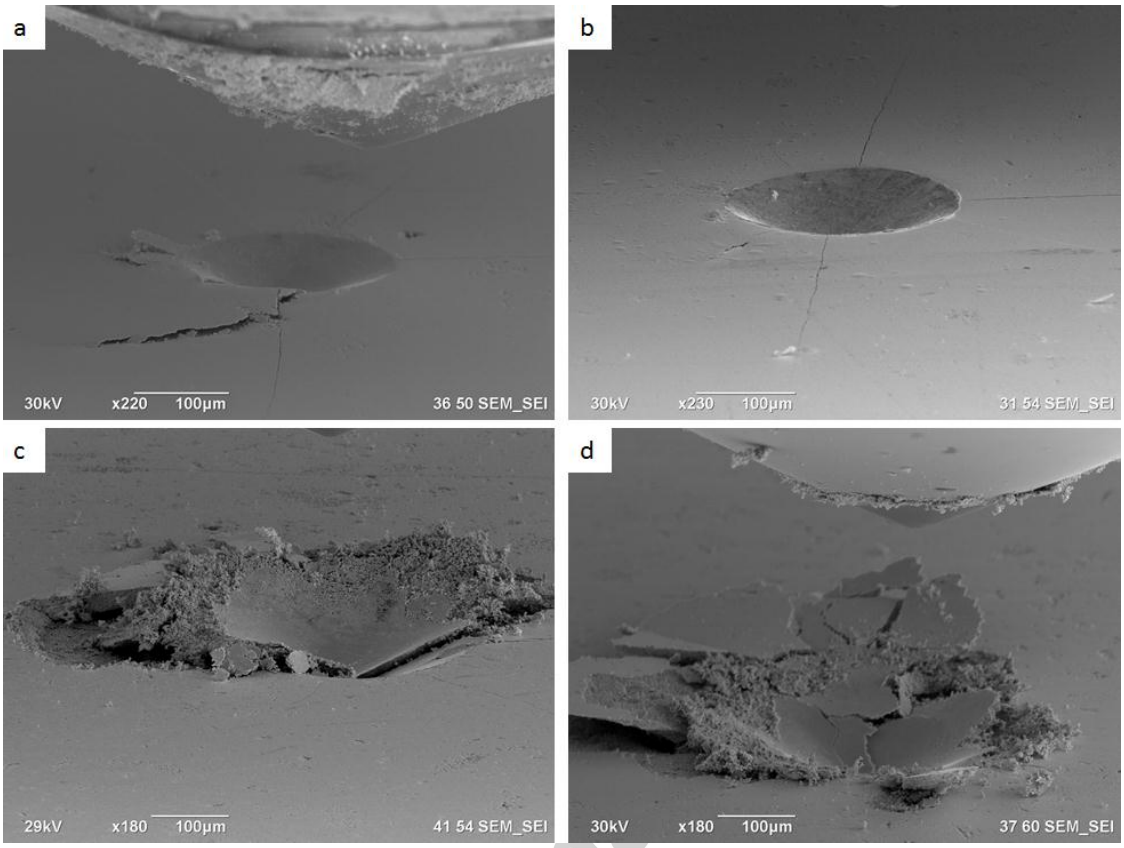

Figure 6. SEM images of residual indents after high-load indentation: (a) pure TaC, (b) TaC-1G, (c) TaC-3G, (d) TaC-5G.

4. Discussion

The load-displacement curves of pure TaC and TaC-5G at high indentation load of 500 N shown in Figure 3 are the direct reflection of the damage behavior of TaC with and without GNPs. Although the final residual displacement (0.4-0.45 μm) in these two samples was similar, their deformation behavior during loading was totally different. As per real time SEM video (video 1, time: 4 sec) grain slipping and lift-off occur in the porous region during loading of pure TaC. TaC has poor sinterability and without sintering aid, it is hard to achieve full densification. Upon application of high external load, the grains in porous areas tend to slide against each other due to the weak bonding. This behavior explains the relatively smaller slope (region marked 1) at

the beginning of loading of pure TaC in load-displacement curve shown in Figure 1. After initial slipping of grains, localized consolidation occurs under the highly stressed region which prevents further sliding and, crack propagation becomes the dominated energy dissipating mechanism. An increase in the slope during loading (region marked 2 in Figure 3) is indicator of the crack propagation. Long cracks (0.5-0.7 mm) were found after the high load indentation test as observed in Figure 5a and Table 2.

The load displacement curve of TaC-5G sample shows greater displacement (0.65 mm) at maximum load of 500 N as compared to pure TaC. Addition of GNP results in lower hardness which results in greater displacement during indentation. The spikes (marked as region 3) in loading curve of TaC-5G sample are attributed to localized events of cracking, as shown in Figure 6d. However, cracks obtained in TaC-5G samples were remarkably shorter than pure TaC sample, thanks to the presence of GNPs. GNPs promote energy dissipation mechanisms through crack deflection as seen in real time indentation video 2 (time 20-40 sec).

The reduction in total residual damage area (Table 2 and Figure 5) with increasing GNPs content is also attributed to the toughening mechanisms introduced by GNPs. TaC-1G had a clean residual indent with an average crack length similar to pure TaC. The toughening effect of GNPs becomes more pronounced with a volume fraction of GNPs above 3%, as observed in Figure 5 and 6c. The residual indent of TaC-3G was much smaller and rougher as compared to pure TaC and TaC-1G, but fewer cracks were visible. The addition of GNPs resulted in 112% reduction in total damage area of TaC-3G as compared to pure TaC. Significant localized damaged with grain sliding is observed for TaC-3G in Figure 6c. TaC-5G indent (Fig 6d) also displayed similar features as TaC-3G but with a smaller damage area. The residual damage area of TaC-5G sample was 580% smaller than pure TaC due to significant reduction in number of

indentation cracks and average crack length. The fact that there was no obvious cracks in TaC-3G and TaC-5G samples indicated GNPs had great ability to restrict damage locally in ceramics.

The role of GNP/TaC interface is important in promoting toughening mechanisms and has been investigated by TEM, as shown in Figures 2d-f. It is generally agreed that interface between reinforcement and ceramic matrix should be well bonded but not so strong that it prevents energy from being dissipated through friction. At the same time, contact between reinforcement and matrix should be maximized to ensure effective transfer of shear stresses. However, the role of interfacial products including amorphous phase formation on interfacial strength is not well studied. Figures 2e-f show mixed kinds of TaC/GNP interfaces with both amorphous and clean interfaces. Ramirez et al. [22] concluded that the presence of defects due to partial oxidation of graphene could lead to formation of glassy phase and the increased mechanical locking. The increased interaction with the glassy phase would indicate that the energy dissipated during de-bonding would be high for GNPs resulting in improvement in fracture toughness. However a thicker layer of reaction product at the interface could weaken the bond and result in delamination [23]. Tightly bonded graphene and TaC grain would not only inhibit grain growth during the SPS process, but also deflecting crack propagation as showing in video 2 (0:20-0:25); a snapshot of which is showed in figure 7. A colorized graphene is shown in Figure 7 for improved visualization. Graphene layer is very thin and transparent showing underlying TaC grain structure. Graphene deflects the crack growth causing a chunk of TaC removal with a release of massive energy is a great evidence that GNP can restrain the crack growth.

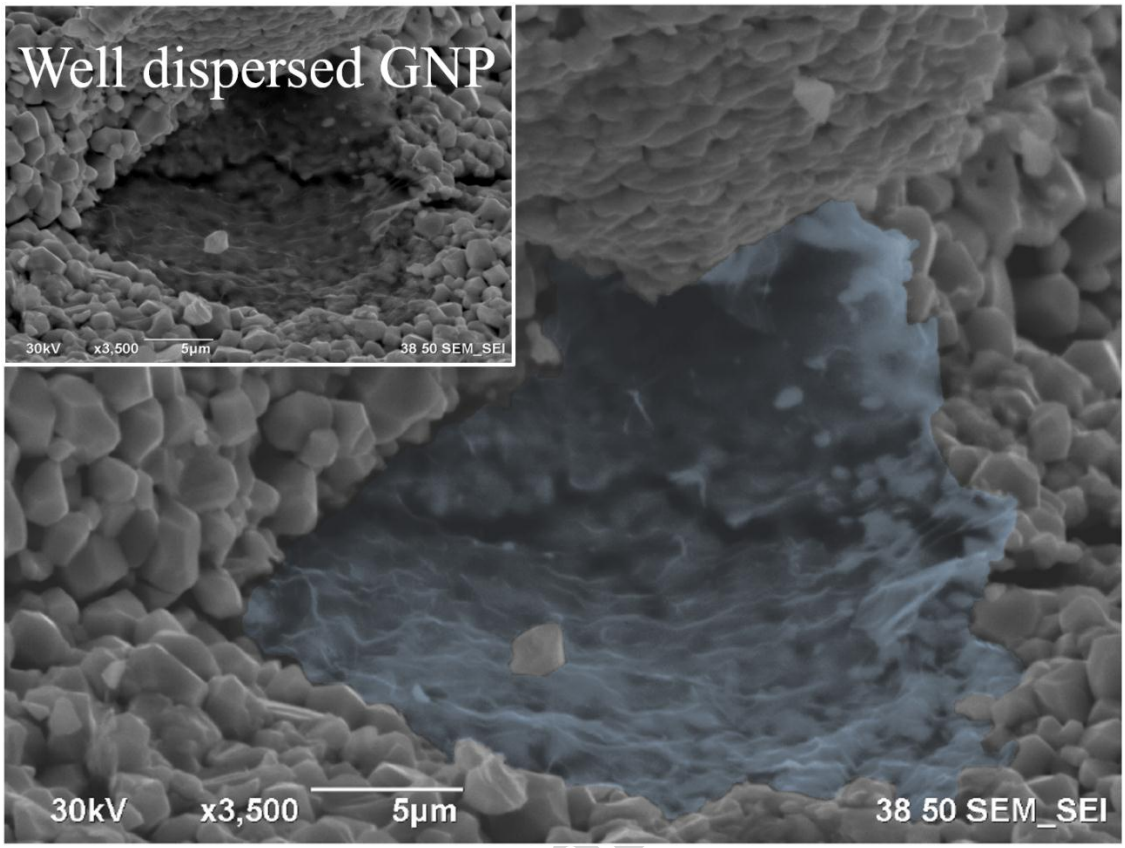

Figure 7. Crack arrest by a thin graphene layer (colored). Initial picture is shown as inset.

5. Conclusions

High load *in-situ* indentation with real-time imaging has proved to be a great tool to analyze deformation response and study damage behavior of GNPs reinforced TaC. The sequence of deformation (e.g. spikes, change in the slope) occurring during the loading and unloading process have been identified and correlated with the microstructure changes. With an increasing GNPs content from 0 to 5 vol.%, TaC-GNP composites, the crack length and total impact (damaged) area of TaC decreased from 26 to 85% respectively. TEM images show that well dispersed GNPs result in a strong and clean interface between TaC and GNP with trace amount of amorphous layer that leads to improved energy dissipation mechanism.

Acknowledgment

The authors acknowledge Dr. Ali Sayir, Program Manager of High Temperature Aerospace Materi-als at the Air Force Office of Scientific Research, and the receipt of Grant FA9550-12-1-0263. The authors also acknowledge the support from the Advanced Materials Engineering Research Institute (AMERI) at Florida International University, Miami, USA.

References

1. W. G. Fahrenholtz, E. J. Wuchina, W. E. Lee, Y. Zhou. Ultra-high temperature ceramics: Materials for extreme environment applications. *John Wiley & Sons, Inc.*, Hoboken, New Jersey. 2014.
2. S. A. Shvab, F. F. Egorov. Structure and some properties of sintered tantalum carbide. *Soviet Powder Metallurgy and Metal Ceramics*. 2011(21): 894-897.
3. L.E. Louis. Transition metal carbides and nitrides. *Academic Press*, New York. 1971.
4. K. Upadhya, J. Yang, W. P. Hoffman. Materials for ultrahigh temperature structural applications. *Am. Ceram. Soc. Bull*., 1997(76): 51-56.
5. L. Silvestroni, D. Sciti. Transmission electron microscopy on Hf- and Ta- carbides sintered with $TaSi_2$. J. *Euro. Ceram Soc. 31* (2011) 3033–3043
6. K. Balani, G. Gonzalez, A. Agarwal, R. Hickman, J.S. O'Dell and S. Seal. Synthesis, microstructural characterization, and mechanical property evaluation of vacuum plasma sprayed tantalum carbide. *J. Am. Ceram. Soc*., 2006 (89): 1419-1425.

7. S.R. Bakshi, V. Musaramthota, D. Lahiri, V. Singh, S. Seal and A. Agarwal. Spark plasma sintered tantalum carbide: Effect of pressure and carbon nanotube addition on microstructure and mechanical properties. *Mater. Sci. Eng. A,* 2011 (528): 2538-2547.
8. S. R. Bakshi, V. Musaramthota, D. Lahiri, V. Singh, S. Seal, A. Agarwal. Spark plasma sintered tantalum carbide: effect of pressure and nano-boron carbide addition on microstructure and mechanical properties. *Mater. Sci. Eng. A,* 2011 (528): 1287-1295.
9. D. Lahiri, V. Singh, G. R. Rodrigues, T. M. H. Costa, M. R. Gallas, S. R. Bakshi, S. Seal, A. Agarwal. Ultrahigh-pressure consolidation and deformation of tantalum carbide at ambient and high temperature. *Acta Mater.*, 2013 (61): 4001-4009.
10. D. Lahiri, E. Khaleghi, S. R. Bakshi, W. Li, E. A. Olevsky, A. Agarwal. Graphene-induced strengthening in spark plasma sintered tantalum carbide-nanotube composite. *Scripta Mater.*, 2013 (68): 285-288.
11. A. Nieto, D. Lahiri, A. Agarwal. Graphene nanoplatelets reinforced tantalum carbide consolidated by spark plasma sintering. *Mater. Sci. Eng. A*, 2013 (582): 338-346.
12. A. Nieto, D. Lahiri, A. Agarwal. Nanodynamic mechanical behavior of graphene nanoplatelet-reinforced tantalum carbide. *Scripta Mater*., 2013 (69): 678-681.
13. L.S. Walker, V.R. Marotto, M.A. Rafiee, N. Koratkar, E.L. Corral. Toughening in graphene ceramic composites. ACS Nano. 2011(5): 3182-3190.
14. M. Belmonte, A. Nistal, P. Boutbien, B. Roman-Manso, M.I. Osendi, P. Miranzo. Toughened and strengthened silicon carbide ceramics by adding graphene-based fillers. Scripta Mater., 2016 (113): 127-130.
15. L. Silvestroni, L. Pienti, S. Guicciardi, D. Sciti. Strength and toughness: the challenging case of TaC-based composites, *Composites: Part B,* 72 (2015) 10-20.].

16. J. D. Nowak, K. A. Rzepiejewska-Malyska, R. C. Major, O. L. Warren. J. Michler. In-situ nanoindentation in the SEM. Materials Today: electron microscopy special issue: 44-45.
17. S. Kiani, C. Ratsch. A. M. Minor, J. M. Yang, S. Kodambaka. In situ transmission electron microscopy observation of room-temperature plasticity in sub-micron-size TaC(100) and TaC(011) single crystals. *Scripta Mater.*, 2015 (100): 13-16.
18. J.M. Wheeler and J. Michler. Elevated temperature, nano-mechanical testing in situ in the scanning electron microscope. *Rev. Sci. Instrum*. 2013(84) 045103
19. J.M. Wheeler, P. Brodard, J. Michler. Elevated temperature, in situ indentation with calibrated contact temperatures. *Philos. Mag.* 2012(25-27): 3128-3141.
20. C. Rudolf, B. Benjamin, A. Agarwal. In situ indentation behavior of bulk multi-layer graphene flakes with respect to orientation. *Carbon*, 2015 (94): 872-878
21. C. Rudolf, B. Boesl, A. Agarwal. In situ mechanical testing techniques for real-time materials deformation characterization. *JOM*. 2016 (68): 136-142
22. C. Ramirez, M.I. Osendi. Toughening in ceramics containing graphene fillers. *Ceram. Int.*, 2014 (40): 11187-11192.
23. Y. Fan, M. Estili, G. Igarashi, W. Jiang, A. Kawasaki, The effect of homogeneously dispersed few-layer graphene on microstructure and mechanical properties of Al_2O_3 nanocomposites. *J. Eur. Ceram. Soc*., 2014 (34): 443-451.